3rd International Structural Specialty Conference
3ième conférence internationale spécialisée sur le génie des structures

Edmonton, Alberta
June 6-9, 2012 / *6 au 9 juin 2012*

Evaluation of Flexural Stiffness for RC Beams During Fire Events

S.F. El-Fitiany[1] and M.A. Youssef[1]
[1] Department of Civil and Environmental Engineering, The University of Western Ontario

Abstract: Analysis of Reinforced Concrete (RC) structures for fire safety is usually conducted at the research level rather than practical design applications. This limitation is due to the complexity of the fire problem and the need for comprehensive finite element tools. Fire performance of RC continuous beams can be predicted by superimposing the effects of thermal expansion and vertical loads. The free thermal rotation of RC sections during fire exposure can be described by the thermal curvature at different fire durations. On the other hand, the reduction in the material mechanical properties can be represented by the degradation in the flexural stiffness of the exposed cross-section. This paper presents a comprehensive parametric study on the reduction of the flexural stiffness for rectangular RC sections heated from three sides according to ASTM-E119 fire exposure. The effective flexural stiffness is determined as the secant slopes of the moment-curvature diagrams. These curves are constructed for heated RC sections at different axial load levels. Based on the results of the parametric study, the authors proposed equations to estimate the reduced flexural stiffness for RC beams at different fire durations up to 2.5 hrs. Structural engineers can use the proposed equations to check the structural fire safety of RC beams.

1. Introduction

Fire impacts Reinforced Concrete (RC) members by raising the temperature of the concrete mass. This rise in temperature significantly reduces the mechanical properties of concrete and steel. Moreover, fire temperatures induce new strains, thermal and transient creep. They might also result in explosive spalling of surface pieces of concrete members. As a result, fire exposed RC members experience a dramatic decrease in their flexural stiffness and thermally deform based on the heating scenario.

The only available approach to predict the behavior of a RC element during a fire event is to conduct a nonlinear coupled thermal-stress Finite Element (FE) analysis. The FE method has proven to be a powerful method to predict the behavior of concrete structures during exposure to fire events. Drawbacks of using the FE method including: the need for a comprehensive computer program, the difficulty to comprehend its results and to identify potential modeling errors, and the long running time make it impractical for design engineers. The complexity of this method becomes obvious in indeterminate structures where different regions of the structure have different heating regimes, cross-section dimensions, reinforcing bars configuration, and axial restrain conditions.

A simplified sectional analysis method to estimate the capacities and deformations of statically determinate RC elements during fire exposure was developed and validated by the El-Fitiany and Youssef (2008). Although this sectional analysis method is relatively easy to apply when compared to the FE method, it still requires knowledge of heat transfer principles and ability to conduct analysis at elevated temperatures.

2. Objectives and Scope

Analysis of RC beams for structural fire safety can only be conducted at the research level and requires long computation time. This limitation is due to the high nonlinearity in the thermal and mechanical properties of concrete at elevated temperatures and the need for comprehensive FE tools. Fire ratings are currently satisfied using prescriptive methods that include specifying the reinforcing steel temperature, the minimum section dimensions, and the minimum required cover. Engineers need simplified tools to predict the behavior of RC structures during a fire event. These tools are also needed by emergency response teams as a quick assessment of the structure integrity to ensure the safety of field members.

In this paper, a number of RC rectangular sections with different cross-section dimensions, reinforcement configuration, material properties, axial restraint level, and preloading levels are analyzed during the standard ASTM-E119 fire exposure. Results of the parametric study are used to provide designers with simplified expressions for the effective flexural stiffness of RC beams subjected to ASTM-E119 fire exposure. These expressions will allow them to have a quick idea about the serviceability of RC beams during fire events.

3. Sectional Analysis at Elevated Temperatures

Fire temperature drastically decreases concrete and steel mechanical properties and induces thermal and transient strains. Total concrete strain at elevated temperatures (ε) is composed of three terms: unrestrained thermal strain (ε_{th}), instantaneous stress related strain (ε_c), and transient creep strain (ε_{tr}). Fire performance of RC beams can be predicted by summing those strain components as shown in Equation 1.

[1] $$\varepsilon = \varepsilon_{th} + \varepsilon_c + \varepsilon_{tr}$$

A sectional analysis approach suitable for the analysis of rectangular RC beams at elevated temperatures was proposed by El-Fitiany and Yousse (2008). Figure 1a shows the fiber model of a typical RC beam cross-section. The shown beam is assumed to be exposed to fire from three sides. The approach can be briefly explained by the following main steps:

- At specific fire duration, a heat transfer analysis is conducted and the temperature distribution through the cross section is predicted. The cross-section is then divided into horizontal layers and two average temperatures, T_σ and T_{th}, are assigned to each layer. T_σ and T_{th} are calculated to represent the average layer strength and the average layer temperature, respectively.

- The nonlinear thermal strain (ε_{th}) distribution, shown in Figure 1f, is calculated using T_{th}. The thermal strain of steel bars is calculated based on the concrete temperature at their location. As bottom bars are usually located at different distances from the concrete surface, different steel thermal strains are calculated as shown in Figure 1f. ε_{th} is then converted to an equivalent linear thermal strain ($\overline{\varepsilon_{th}}$) by considering self equilibrium of internal thermal forces in concrete and steel layers, Figure 1. The linear distribution is characterized by the unrestrained thermal axial strain, ε_i, and curvature, ψ_i. Figure 1e shows the differences between the equivalent linear and nonlinear thermal strains which

represent the self induced thermal strains (ε_{st}). These strains are assigned as initial strains for the concrete and steel layers to model the corresponding self-induced thermal stresses at a given point of the fire temperature-time curve. The total strain (ε) can be described as follows

[2] $\varepsilon = \overline{\varepsilon_{th}} + \varepsilon_{st} + \varepsilon_c + \varepsilon_{tr}$

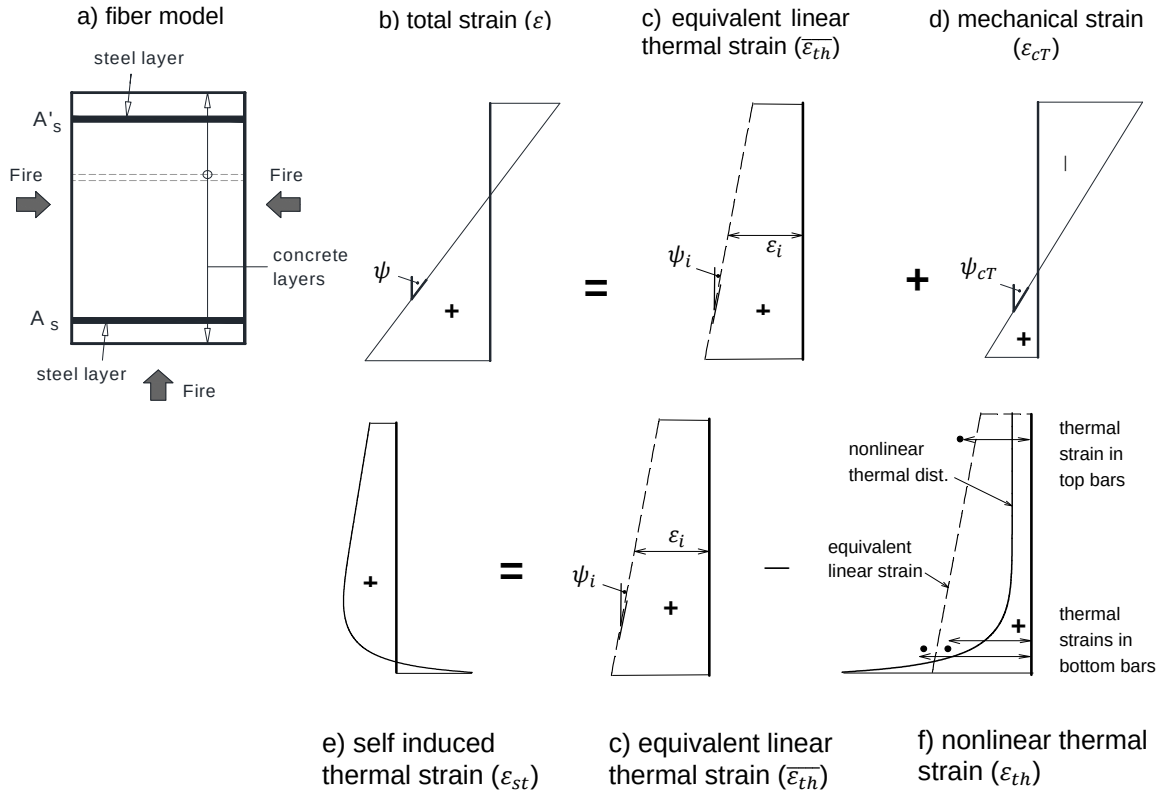

Figure 1: Modified sectional analysis approach for RC sections exposed to fire

- Youssef and Moftah (2007) proposed constitutive stress-strain relationships for concrete and steel which implicitly accounts for the transient creep ε_{tr}. The instantaneous stress related strain(ε_c), self induced thermal strain (ε_{st}), and the transient strain (ε_{tr}) terms are lumped in a mechanical strain term (ε_{cT}). ε_{ct} is then added to ε_i to calculate total effective strain ε. Equation 2 can be rewritten as follows

[3] $\varepsilon = \overline{\varepsilon_{th}} + \varepsilon_{cT}$

- Using the concrete and steel constitutive relationships that is based on T_σ, the corresponding stress is calculated. By considering the equilibrium of the stresses developed in all of the layers, the corresponding moment can be calculated. The behavior of the analyzed cross-section is presented by moment (M)–curvature (ψ) diagram.

4. Moment-Curvature Relationships of Fire-Heated Sections

In this section, characteristics of M–ψ relationships are discussed. Figure 2 shows schematics for the M–ψ curves for RC sections subjected to sagging and hogging moments. The end point on the curve defines the nominal moment capacity (M_n) that corresponds to the curvature capacity of

the analyzed cross-section. The secant slope of the M–ψ diagram represents the cross-section's stiffness at a specific moment (M_{app}) or act at specific applied load level (λ), where $\lambda = M_{app}/M'_n$. M'_n is the nominal flexural capacity at ambient temperature.

Considering an assumed fire duration, it can be stated that the effect of thermal strain on the M–ψ relationship is constant regardless of the load level. This constant effect describes the free thermal expansion of the unloaded concrete element. It results in shifting the M–ψ diagram by a value ψ_i that can be predicted by calculating the nonlinear thermal strain distribution and converting it to an equivalent linear distribution as discussed earlier in this paper. The $M-\psi$ diagram includes the effects of material degradation, transient creep strain (ε_{tr}), and self induced thermal strain (ε_{st}). The total curvature (ψ) is the sum of the unrestrained thermal curvature (ψ_i) and the mechanical curvature (ψ_{cT}) and can be expressed in terms of the effective stiffness (EI_{eff}) as follows.

[4] $\psi = \psi_i + M_{app}/EI_{eff}$

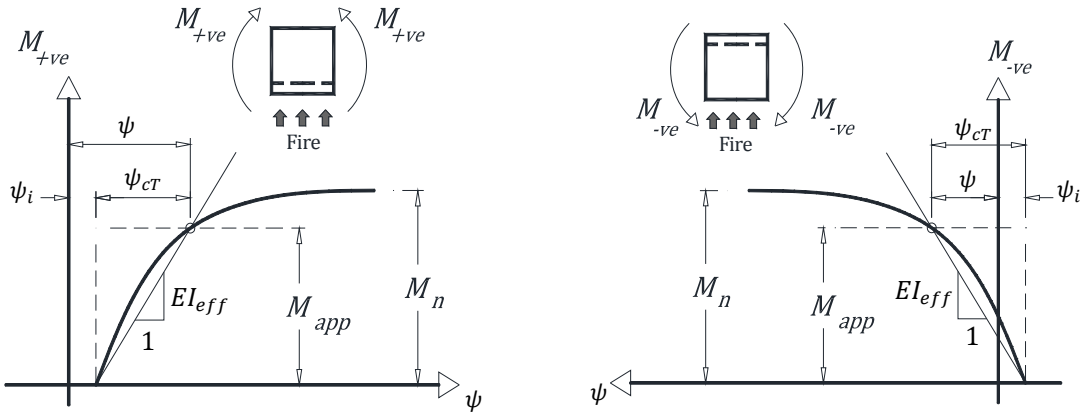

a) sagging moments (M_{+ve}) b) hogging moments (M_{-ve})

Figure 2: (M)–(ψ) diagrams for RC beams during fire

As shown in Figure 2, heating RC beams from the bottom face and the two sides cause the lower concrete fibers to thermally expand more than the upper concrete fibers and results in ψ_i. Consequently, the acting moment induces a mechanical curvature (ψ_{cT}) which will either be added to ψ_i or counteract with it. Figure 2 illustrates the effect of applying positive (sagging) moments, induces a curvature in the same direction as ψ_i, and negative (hogging) moments, results in a curvature in the opposite direction of ψ_i.

5. Evaluation of Effective Flexural Stiffness

In this section, the effects of different geometric and material factors on the effective flexural stiffness (EI_{eff}) are discussed using a comprehensive parametric study. The study aims at providing structural engineers with simple expressions to evaluate this parameter without the need for heat transfer and sectional analysis calculations.

Table 2 summarizes the properties of the analyzed beams. All the beams have rectangular cross-section and are subjected to ASTM-E119 standard fire exposure from three sides as shown in Figure 3. The considered parameters are width (b), height (h), concrete compressive strength (f'_c), flexural moment at ambient temperature ($\lambda = 30\% - 60\%$), axial load level at ambient

Table 1: Parametric study cases

Beam #	b (mm)	h (mm)	f'_c (MPa)	λ	λ_p	n	Agg	$\rho'\%$ (A_g)	$\rho\%$ (A_g)
B1	300	500	30	0.15 , 0.30 , 0.45 , 0.60	0.00	1	siliceous	0.13	0.5
B2									1.0
B3						2			1.5
B4									2.5
B5	300	700			0.00	1	siliceous	0.10	0.5
B6						2			1.0
B7									1.5
B8									2.5
B9	400	700			0.00	2	siliceous	0.07	1.0
B10									2.5
B11	500	700			0.00	2	siliceous	0.06	1.0
B12									2.5
B13	300	300			0.00	1	siliceous	0.22	1.5
D1	300	500	20	0.45	0.00	1	siliceous	0.13	0.5
D2									1.0
D3						2			1.5
D4									2.5
D5	300	700	40	0.45	0.00	1	siliceous	0.10	0.5
D6						2			1.0
D7									1.5
D8									2.5
D9	400	700	50	0.45	0.00	2	siliceous	0.07	1.0
D10									2.5
D11	500	700	50	0.45	0.00	2	siliceous	0.06	1.0
D12									2.5
I1	300	500	30	0.45	0.00	1	siliceous	0.13	0.5
I2							carbonate	0.13	1.0
I4	300	700	40	0.45	0.00	2	siliceous	0.25	1.0
I5								0.45	
I6								0.65	
I7	300	700	40	0.45	0.00	2	carbonate	0.10	1.5
I8	300	700	40	0.45	0.00	2	siliceous	0.10	1.0
I9								0.10	
I10	400	700	50	0.45	0.00	2	siliceous	0.15	2.5
F1	300	500	30	0.45	0.1, 0.2, 0.3	2	siliceous	0.13	1.5
F2	300	500	30	0.60		2	siliceous	0.13	1.5
F3	300	700	30	0.30		2	siliceous	0.10	2.5

temperature ($\lambda_p = 0.0\% - 30\%$), number of tensile steel layers ($n = 1, 2$), aggregate type (Agg), compression reinforcement ratio ($\rho' = 0.06\% - 0.65\%$), and tensile reinforcement ratio ($\rho = 0.5\% - 2.5\%$). The standard reinforcement layout, shown Figure 3, is assumed in this study. The parametric study is limited to siliceous and carbonate concretes with compressive strength (f'_c) ranging between 20 and 50 MPa . The fire duration (t) ranges from 0.0 to 2.5 hr.

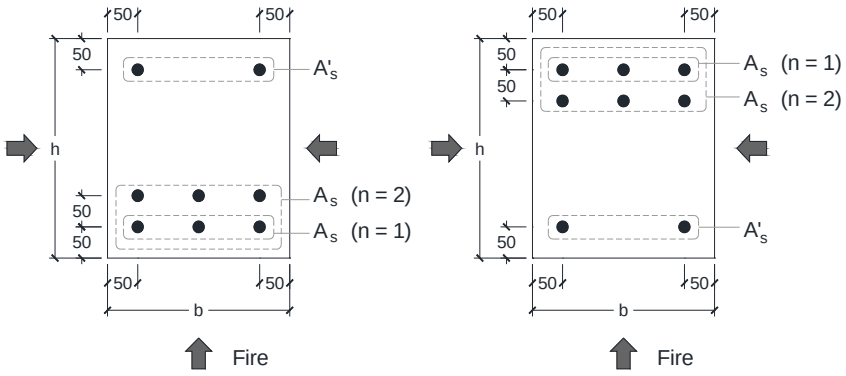

a) sagging moments (M_{+ve}) b) hogging moments (M_{-ve})

Figure 3: Typical cross-sections for the parametric study beams (Dimensions in mm)

5.1 Analysis and discussion

Using the obtained moment – curvature relationships, the secant slope (EI_{eff}) is evaluated at four load levels, $\lambda = 15\%, 30\%, 45\%,$ and 60%, for different fire durations. Figures 4 - 7 show the effect of ASTM-E119 fire exposure on the flexural stiffness, as a ration from the ambient gross flexural stiffness ($E_c I_g$), for a number of studied rectangular RC beams considering the cases of positive and negative moments. The effect of different parameters on EI_{eff} is discussed below.

5.1.1 Effect of tensile reinforcement ratio (ρ)

Figure 4 shows the effect of ρ on the effective flexural stiffness (EI_{eff}). Similar to ambient temperature, EI_{eff} of RC beams is mainly dependant on the tensile reinforcement ratio (ρ). Fire temperature severely affects the yielding strength of tensile reinforcing bars especially for the case of positive moment when tensile steel bars are heated from two adjacent sides simultaneously, Figure 4. For the case of negative moment, the significant reduction of the concrete compressive strength, located adjacent to the fire side, decreases the effective section height. This reduction in the concrete strength is indicated in Figure 4, case of M-ve, by the sudden drop in EI_{eff} values rather than gradual reduction in EI_{eff} due to the heating of tensile reinforcing bars, i.e. case of M+ve. For the case of negative moment, the tensile reinforcing bars are located at the top of the sections and their effect on EI_{eff} becomes less significant compared to the case of positive moment as shown in Figure 4.

5.1.2 Effect of preloading level (λ)

Figure 5 shows the effect of the preloading level (λ) on the effective flexural stiffness (EI_{eff}). As the tensile resistance of concrete is neglected in the sectional analysis methodology, the effect of the λ on EI_{eff} is minor.

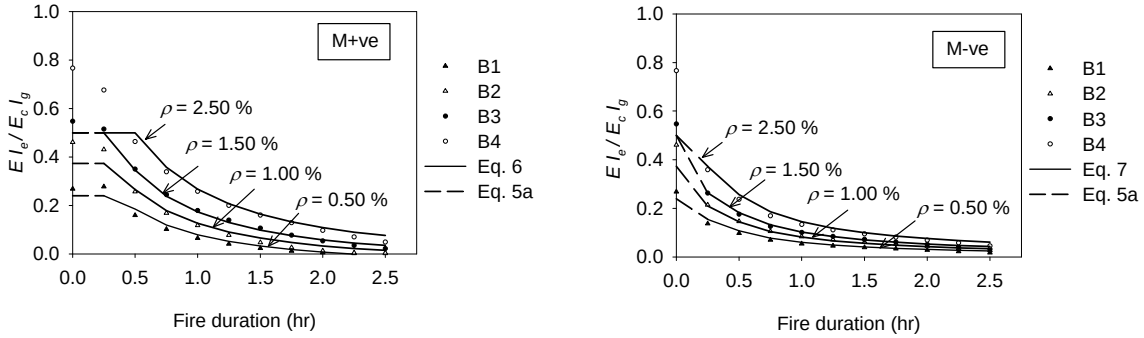

Figure 4: Effect of tensile reinforcement ratio ρ on EI_{eff}

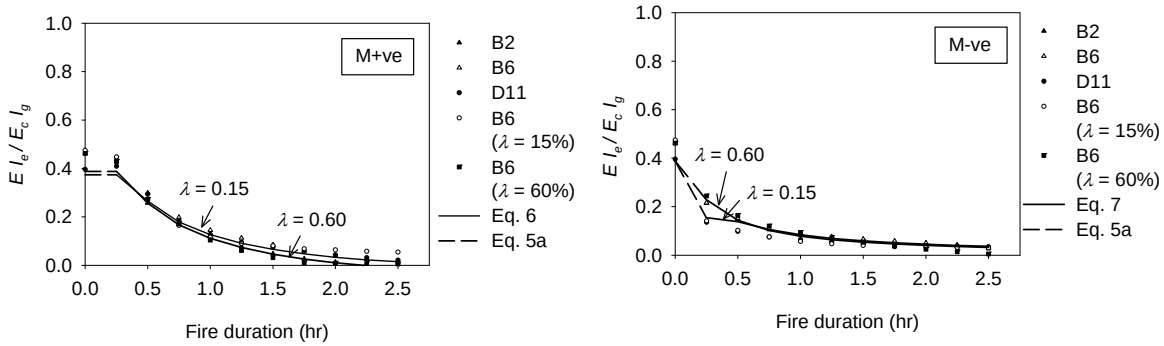

** λ = 45 % (unless mentioned)

Figure 5: Effect of section dimensions (b, h) and compressive strength (f'_c) on EI_{eff}

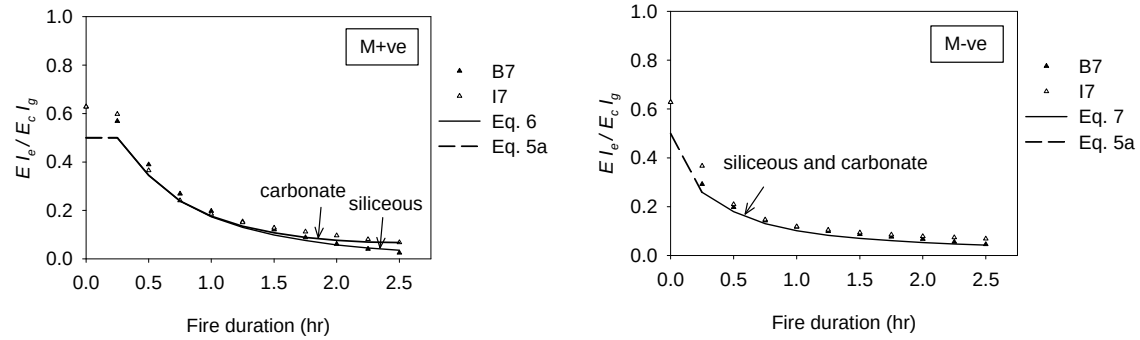

Figure 6: Effect of aggregate type (Agg) on EI_{eff}

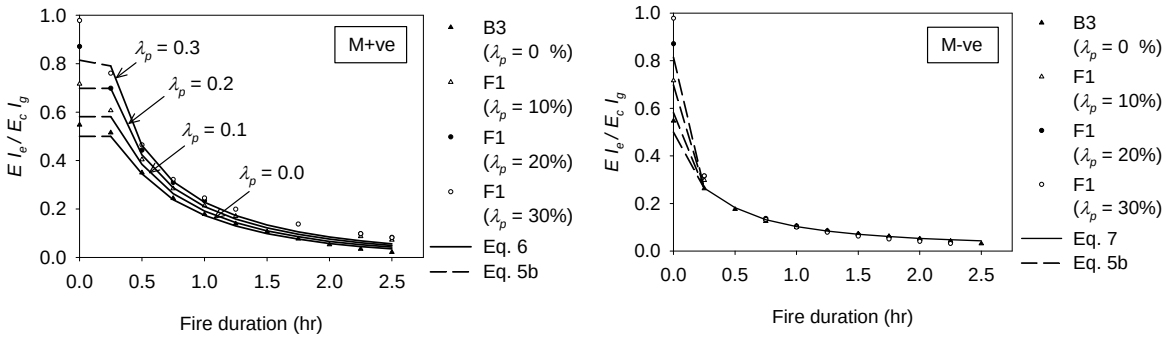

Figure 7: Effect of axial load level (λ_P) on EI_{eff}

5.1.3 Effect of section dimensions (b, h), compressive strength (f'_c), and aggregate type (Agg)

Figures 5 and 6 show the variation of EI_{eff} with fire duration for beams with different cross-section dimensions, concrete compressive strengths, and aggregate types. As shown in Figures 5 and 6, their results are found to overlap which indicates that these factors have a negligible effect on the stiffness degradation.

5.1.4 Effect of axial restrain level (λ_P)

The effect of the applied axial load is shown in Figure 7. In this figure, λ_P represents the ration between the applied axial load and the axial capacity at ambient temperature. As shown in Figure 7, changing the axial restrain level (λ_P) has a considerable effect on EI_{eff} at ambient temperature. However, its effect is minimized during fire exposure.

5.2 Proposed expressions for the effective flexural stiffness EI_{eff}

The effective flexural stiffness at ambient temperature can be estimated using the equations developed by Khuntia and Ghosh (2004) which were developed based on their analytical study. These equations are slightly modified by the ACI 318-08. The ratio between EI_{eff} and the stiffness of the uncracked flexural stiffness ($E_c I_g$) at ambient temperature can be evaluated using Equation 5a, for sections subjected to pure flexure, and Equation 5b, for sections subjected to combined flexure and axial force.

[5a] $$EI_{eff}/E_c I_g = (0.10 + 0.25 \times \rho)\left(1.2 - 0.2 \times \frac{b}{d}\right) \quad \leq \quad 0.5$$

[5b] $$EI_{eff}/E_c I_g = \left(0.80 + 0.25 \times \rho_g\right)(0.3 + 0.5 \times \lambda_u) \quad \leq \quad 0.875$$

Where,

EI_{eff} is the effective flexural stiffness at ambient temperature (i.e. $t = 0.0\ hrs$)

E_c is the secant modulus for concrete and can be evaluated in MPa as $4500\sqrt{\mathrm{f'_c}}$

f'_c concrete compressive strength in MPa

I_g gross sectional second moment of inertia

b is the cross-section width in mm

d is the effective depth of tensile reinforcement in mm

ρ percentage of tensile reinforcement relative to $(\mathrm{b} \times \mathrm{d})$

ρ_g percentage of gross reinforcement relative to $(\mathrm{b} \times \mathrm{d})$. For beams, $\rho_g \cong 2 \times \rho$

λ_u ratio between factored axial load and the nominal axial capacity, $\lambda_u \cong 1.5 \times \lambda$

During ASTM-E119 fire exposure, Equations 6 and 7 are proposed to predict the degradation of EI_{eff} for sections subjected to positive and negative moments, respectively. These equations are developed based on a multiple regression analysis of the parametric study results, Figure 8.

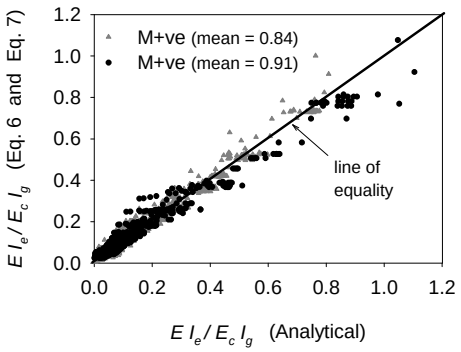

Figure 8: Regression analysis of EI_{eff}

[6] $$EI_{eff}/E_cI_g = 2.032 \times 10^{-2} - \left(0.180 + 1.408 \times \rho - 1.3047 \times \lambda_p\right) \times {}^{1}/_{t^2} \times 10^{-2}$$

$$+\left(5.897 + 10.806 \times \rho + 16.864 \times \lambda_p\right) \times {}^{1}/_{t} \times 10^{-2} + (2.590 \times \lambda + 0.651 \times Agg) \times t^2 \times 10^{-2} - (12.676 \times \lambda + 0.375 \times Agg) \times t \times 10^{-2}$$

[7] $$EI_{eff}/EI_g = -0.210 \times 10^{-2} - (1.329 + 0.506 \times \rho - 1.762 \times \lambda - 0.14 \times \rho') \times 1/t^2 \times 10^{-2}$$

$$+(5.414 + 4.2 \times \rho' - 2.948 \times \lambda + 4.747 \times \rho) \times 1/t \times 10^{-2}$$

Where,

t is the ASTM-E119 fire duration in hrs ($\mathrm{t} \geq 0.25\ \mathrm{hr}$)

Agg is a factor to account for the aggregate type (0.0 for siliceous concrete and 1.0 for carbonate concrete)

λ is the flexural level at ambient temperature

λ_P is the axial load level (restrain effect)

Summary and Conclusions

A sectional analysis methodology was proposed by the authors in previous publications. The application of this methodology is reviewed in this paper. A practical terminology based on superimposing the thermal expansion effect and effective stiffness degradation is proposed. The nonlinear thermal expansion is converted to an equivalent uniform thermal distribution which can be represented by the unrestrained thermal curvature ψ_i. The degradation effect in material strength is considered by accounting for the reduction in the effective flexural strength (EI_{eff}).

A comprehensive parametric study is conducted to investigate the effect of different material, geometric, and loading factors on the unrestrained thermal parameter (ψ_i) and the effective flexural strength (EI_{eff}). For simplicity, the parametric study is limited to rectangular RC beams subjected to $2.5\ hr$ ASTM-E119 standard fire exposure and typical reinforcement configurations. Based on the results of the parametric study, a number of expressions are proposed to predict ψ_i and EI_{eff} for sections subjected to both sagging (positive) and hogging (negative) moments. Designers can apply the proposed methodology using these expressions to conduct a quick assessment for the structural fire safety of RC continuous beams. The proposed equations are only valid for the cross-sections covered in the parametric study.

Acknowledgments

This research was funded by the Natural Sciences and Engineering Research Council of Canada (NSERC).

References

Lie, T.T., ed., "Structural Fire Protection," *ASCE Manuals and Reports on Engineering Practice*, no. 78, New York, NY, 1992, 241 pp.

El-Fitiany, S., Youssef, M.A. 2009, "Assessing the flexural and axial behaviour of reinforced concrete members at elevated temperatures using sectional analysis", *Fire Safety Journal*, vol. 44, no. 5, pp. 691-703.

Youssef, M.A. and Moftah, M., "General stress-strain relationship for concrete at elevated temperatures," *Engineering Structures*, vol. 29, no. 10, 2007, pp. 2618-2634.

Kodur, V.K.R., and Dwaikat, M., "Performance-based fire safety design of reinforced concrete beams," *Journal of Fire Protection Engineering*, vol. 17, no. 4, 2007, pp. 293-320.

El-Fitiany, S.F., and Youssef, M.A., "Stress Block Parameters for Reinforced Concrete Beams During Fire Events," *Innovations in Fire Design of Concrete Structures*, ACI SP-279, 2011, pp. 1-39.

Cement Association of Canada, "Concrete design handbook, CAN/CSA A23.3-04," 3rd Ed., Ottawa, 2006.

Ronald J. Wonnacott. & Wonnacott, Thomas H., 1985 (fourth edition), "Introductory statistics", *New York: John Wiley & Sons*.

Khuntia, M., and Ghosh, S. K., 2004, "Flexural Stiffness of Reinforced Concrete Columns and Beams: Analytical Approach," *ACI Structural Journal*, V. 101, No. 3, May-June, pp. 351-363.

ACI Committee 318,"Building Code Requirements for Structural Concrete (ACI 318-08) and Commentary," *American Concrete Institute*, Farmington Hills, MI, 2005, 465 pp.